LETTERS

Gli3 and *Plzf* cooperate in proximal limb patterning at early stages of limb development

Maria Barna[1,2], Pier Paolo Pandolfi[3,4] & Lee Niswander[2,5]

The vertebrate limb initially develops as a bud of mesenchymal cells that subsequently aggregate in a proximal to distal (P–D) sequence to give rise to cartilage condensations that prefigure all limb skeletal components[1]. Of the three cardinal limb axes, the mechanisms that lead to establishment and patterning of skeletal elements along the P–D axis are the least understood. Here we identify a genetic interaction between *Gli3* (GLI-Kruppel family member 3) and *Plzf* (promyelocytic leukaemia zinc finger, also known as *Zbtb16* and *Zfp145*), which is required specifically at very early stages of limb development for all proximal cartilage condensations in the hindlimb (femur, tibia, fibula). Notably, distal condensations comprising the foot are relatively unperturbed in *Gli3*$^{-/-}$;*Plzf*$^{-/-}$ mouse embryos. We demonstrate that the cooperative activity of *Gli3* and *Plzf* establishes the correct temporal and spatial distribution of chondrocyte progenitors in the proximal limb-bud independently of known P–D patterning markers and overall limb-bud size. Moreover, the limb defects in *Gli3*$^{-/-}$;*Plzf*$^{-/-}$ embryos correlate with the transient death of a specific subset of proximal mesenchymal cells that express bone morphogenetic protein receptor, type 1B (*Bmpr1b*) at the onset of limb development. These findings suggest that the development of proximal and distal skeletal elements is distinctly regulated early during limb-bud formation. The initial division of the vertebrate limb into two distinct molecular domains is consistent with fossil evidence indicating that the upper and lower extremities of the limb have different evolutionary origins[2].

The basic adult pattern of the vertebrate limb skeleton derives from a cartilaginous model: a single proximal long bone within the stylopod segment (humerus; femur), followed by two long bones within the zeugopod segment (radius, ulna; tibia, fibula) and then the distal autopod segment comprising of wrist or ankle, and digits. This initial cartilage pattern is preceded by *Sox9* expression, which marks the chondrocyte precursors of all three segments[3,4]. Several factors, such as *Hox* genes or fibroblast growth factor (*Fgf*) genes, elaborate this initial cartilage pattern either by driving proliferation of specific limb segments along the P–D axis once they are established[5,6] (*Hox*), or by ensuring that there are adequate numbers of mesenchymal cells in the limb-bud to form skeletal elements of the correct size[7] (*Fgf*). However, these mouse mutants display a relatively unperturbed initial cartilage pattern, as revealed by alcian-blue staining[5,6] or *Sox9* expression, which is initially evident in all three P–D segments despite drastically reduced limb-bud size[7]. For example, *Hoxd11*$^{-/-}$;*Hoxa11*$^{-/-}$ mice exhibit a specific loss of the forelimb zeugopod element: the initial cartilage elements comprising the radius and ulna form, but subsequent development is perturbed[5,6]. On the other hand, mutations in genes that affect chondrogenesis, such as *Sox9*, affect the formation of all chondrogenic elements[4]. Therefore, the mechanisms that regulate early events underlying P–D limb patterning are largely unknown.

Here we identified a cooperative role of two transcription factors, *Gli3* and *Plzf*, in the regulation of proximal limb development. *Gli3*$^{-/-}$;*Plzf*$^{-/-}$ double-knockout embryos (see Methods) display a phenotype distinct from the anterior to posterior limb-patterning defects observed in either single mutant[8–10] (Supplementary Fig. 1). All proximal skeletal structures of *Gli3*$^{-/-}$;*Plzf*$^{-/-}$ hindlimbs are severely affected, whereas the distal autopod skeleton is relatively unperturbed (Fig. 1 and Supplementary Fig. 1). Severely affected *Gli3*$^{-/-}$;*Plzf*$^{-/-}$ hindlimbs have only a single piece of proximal

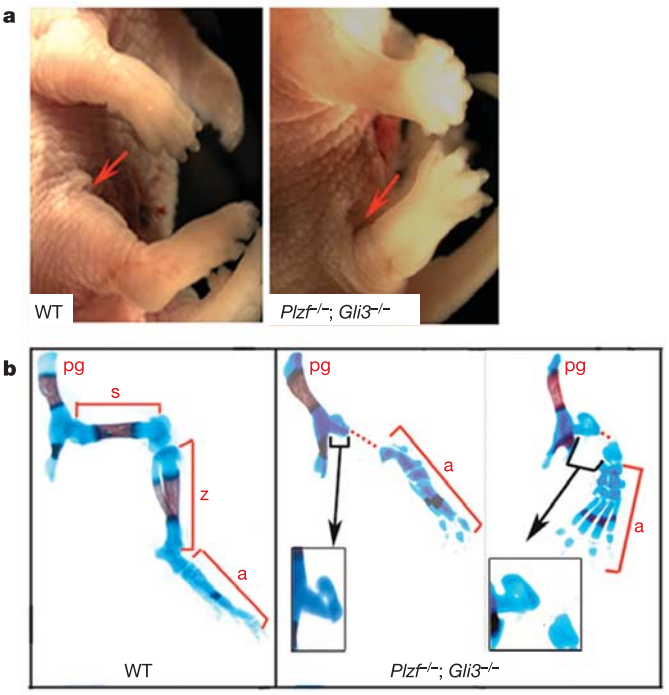

Figure 1 | *Plzf* and *Gli3* regulate proximal skeletal patterning. a, External morphology of E16.5 wild-type (WT) and *Plzf*$^{-/-}$;*Gli3*$^{-/-}$ embryos. Red arrow indicates where hindlimb meets the body wall. **b**, Skeleton of E16.5 hindlimbs demonstrating severe stylopod and zeugopod defects in *Gli3*$^{-/-}$;*Plzf*$^{-/-}$ embryos. Two *Gli3*$^{-/-}$;*Plzf*$^{-/-}$ examples illustrate the most severe phenotype (left) with a single proximal cartilage element and the milder phenotype (right) with two proximal cartilage pieces. In both cases, the proximal element attached to the pelvic girdle (pg) resembles a malformed knee joint. Dashed red line denotes a gap between skeletal elements. The pelvic girdle, which is not derived from the hindlimb bud, appears normal. a, autopod; s, stylopod; z, zeugopod.

[1]Molecular Biology Program, Weill Graduate School of Medical Sciences of Cornell University, New York, New York 10021, USA. [2]Developmental Biology Program, [3]Cancer Biology and Genetics Program, and [4]Department of Pathology, Sloan-Kettering Institute, New York, New York 10021, USA. [5]Howard Hughes Medical Institute and Department of Pediatrics, Section of Developmental Biology, University of Colorado Health Science Center Fitzsimmons Campus, Aurora, Colorado 80045, USA.

cartilage (1 embryo of 12 analysed) that morphologically resembles a malformed knee joint (Fig. 1b). Other representative *Gli3*$^{-/-}$;*Plzf*$^{-/-}$ hindlimbs have variable numbers (2–5) of small pieces of proximal cartilage, which lack the morphology of stylopod and zeugopod elements (Fig. 1b and Supplementary Fig. 1; 11/12). These proximal structures are small, amorphous pieces of cartilage, with the notable exception of a consistent structure resembling an apparent knee joint that is often fused to the pelvic girdle. Despite these proximal defects, the autopod is present and similar to *Gli3*$^{-/-}$ embryos. However, digit number is often reduced to four digits, and there is partial rescue in the overall shape or size of tarsal elements and phalange 1 compared to *Gli3*$^{-/-}$ hindlimbs (Supplementary Fig. 1 and Fig. 1a). Frequently, the calcaneus, an ankle bone, is elongated proximally in *Gli3*$^{-/-}$;*Plzf*$^{-/-}$ hindlimbs (Supplementary Fig. 1; 8/12). There are no discernible P–D skeletal defects in *Gli3*$^{-/-}$;*Plzf*$^{-/-}$ forelimbs (data not shown); however, the embryos die before birth, as do *Gli3*$^{-/-}$ single mutants[10]. We therefore conclude that *Gli3* and *Plzf* specifically cooperate in the development of the hindlimb stylopod and zeugopod.

We determined when these skeletal defects become apparent by examining the earliest cartilage pattern by alcian-blue staining at embryonic day (E) 12.5. *Gli3*$^{-/-}$ or *Plzf*$^{-/-}$ single-mutant hindlimbs show a wild-type cartilage pattern, except for extra digit condensations in *Gli3*$^{-/-}$ embryos (Supplementary Fig. 1). In contrast, although *Gli3*$^{-/-}$;*Plzf*$^{-/-}$ hindlimbs show a relatively normal autopod, morphologically discernible stylopod and zeugopod elements are not apparent (Fig. 2, top panels). Instead, in all E12.5 *Gli3*$^{-/-}$;*Plzf*$^{-/-}$ hindlimbs, a single ball of proximal cartilage is present that does not possess the elongated long-bone morphology characteristic of either the stylopod or zeugopod. The cartilage ball is initially located at the approximate position of the knee joint, coincident with proximal joint formation in wild-type limbs, and at E16.5 an apparent knee joint is present in all *Gli3*$^{-/-}$;*Plzf*$^{-/-}$ hindlimbs (Fig. 1b), although it often fuses to the pelvic girdle. This shift in relative position may result from the absence of proximal long-bone cartilage elements during limb outgrowth. Therefore, we examined expression of joint-specific markers. In E12.5 wild-type hindlimbs, joint markers are expressed in a horseshoe-like stripe where the developing knee joint forms to delineate the area between stylopod and zeugopod (Fig. 2, middle panels), and these cells co-express the cartilage marker collagen, type IIa (*Col2a*). The *Gli3*$^{-/-}$;*Plzf*$^{-/-}$ limbs also express the joint-specific markers *Gdf5*, *Wnt9a* and *Fgf18*, but these markers entirely encompass the single *Col2a*-positive and the alcian-blue-stained proximal ball of cells (Fig. 2, middle panels; data not shown). By E14.5, the proximal cartilage ball in *Gli3*$^{-/-}$;*Plzf*$^{-/-}$ limbs frequently separates into one or more pieces, each of which retains expression of joint markers and *Col2a*, whereas joint markers are expressed between the *Col2a* domains in wild-type limbs (Fig. 2, bottom panels; Supplementary Fig. 2; data not shown). Joint precursors and other mesenchymal derivates, such as tendon, are not initially expanded in *Gli3*$^{-/-}$;*Plzf*$^{-/-}$ limbs at E11.5 (Supplementary Fig. 2 and data not shown) and are expressed in a region similar to that observed in wild-type limbs, indicating that proximal skeletal elements are not misdirected towards a joint or tendon fate. We therefore conclude that formation of the stylopod and zeugopod, but not the proximal joint, is specifically disrupted at very early stages of limb development in *Gli3*$^{-/-}$;*Plzf*$^{-/-}$ embryos.

Histology of *Gli3*$^{-/-}$;*Plzf*$^{-/-}$ limbs showed no evidence of mesenchymal condensation other than the single cartilage ball that expresses joint markers and the autopod at E12.5 (Fig. 3a), and no condensations between separated proximal cartilage pieces at E14.5 (data not shown). Even at the time when wild-type stylopod/zeugopod condensations are first initiated, there is no

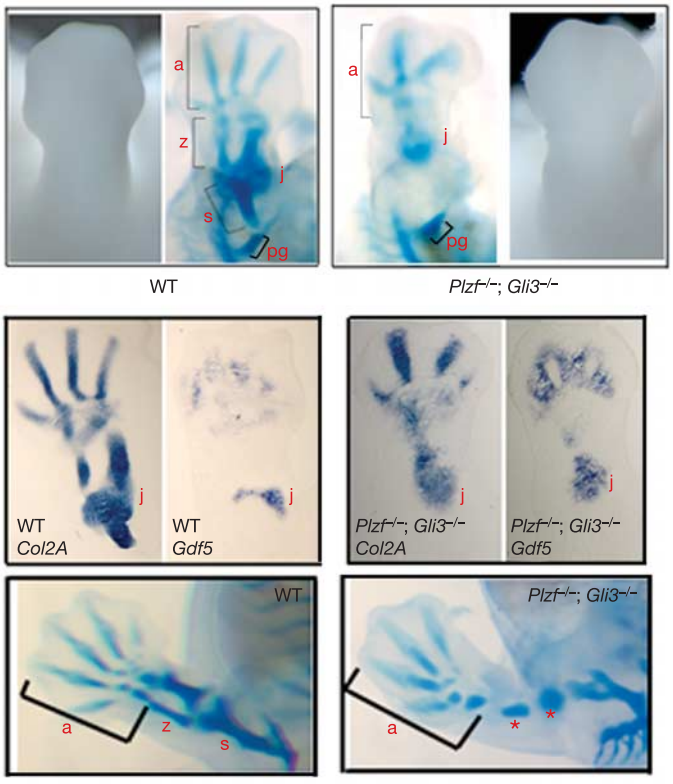

Figure 2 | *Plzf* and *Gli3* regulate molecular and morphological features of the proximal stylopod and zeugopod. Upper panels, E12.5 wild-type and *Gli3*$^{-/-}$;*Plzf*$^{-/-}$ hindlimbs photographed and then stained with alcian-blue to reveal the skeleton. Middle panels, *in situ* hybridizations on hindlimb sections at E12.5 for markers of cartilage (*Col2a*) and joint (*Gdf5*). Lower panels, E14.5 hindlimbs stained with alcian-blue. Asterisks indicate the cartilage pieces that would also express joint markers. j, joint.

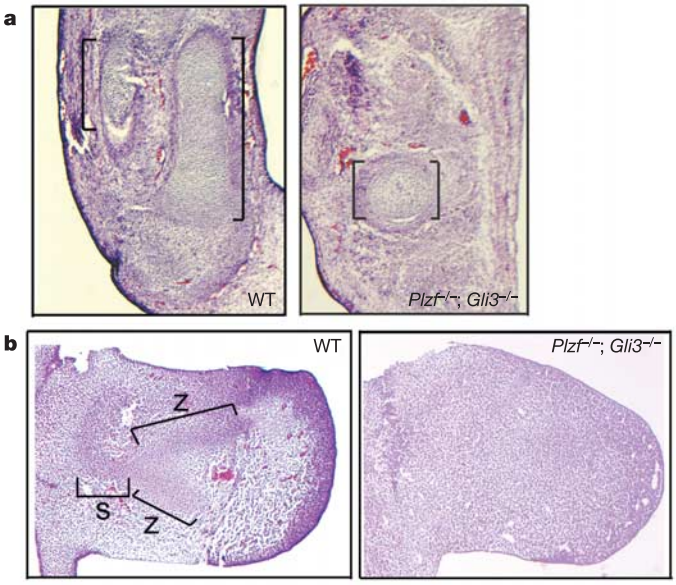

Figure 3 | *Plzf* and *Gli3* are for required for proximal limb condensations. **a**, **b**, Histology of wild-type and *Plzf*$^{-/-}$;*Gli3*$^{-/-}$ hindlimb sections at E12.5 (**a**) and E11.5 (**b**) stained with haematoxylin and eosin. **a**, E12.5 *Gli3*$^{-/-}$;*Plzf*$^{-/-}$ limbs show only a single ball of mesenchymal condensation within the proximal region, which lacks the long-bone morphology of wild-type proximal skeletal elements indicated by brackets. **b**, E11.5 *Gli3*$^{-/-}$;*Plzf*$^{-/-}$ limbs have no discernible chondrogenic mesenchymal condensations.

evidence of proximal condensations in *Gli3*$^{-/-}$;*Plzf*$^{-/-}$ limbs (Fig. 3b), although a half-day later a digit condensation is formed (Supplementary Fig. 3). This raises the question of whether *Plzf* and *Gli3* act at or before the condensation stage to regulate proximal skeletal development.

We therefore examined the earliest-known marker for cartilage differentiation, *Sox9* (refs 3, 4), which is expressed one day before initiation of limb cartilage condensations. Remarkably, at a time when *Sox9* expression is normally initiated in wild-type embryos, there is no *Sox9* expression in *Gli3*$^{-/-}$;*Plzf*$^{-/-}$ hindlimbs (Fig. 4a). At E11.5, *Sox9* is expressed normally in the *Gli3*$^{-/-}$;*Plzf*$^{-/-}$ autopod, consistent with its formation in mutant hindlimbs. However, in proximal regions there is only a small clump of *Sox9*-positive precursors (Fig. 4a), which may correspond to the later proximal cartilage piece revealed by histology, alcian-blue staining and joint marker expression at E12.5 (Figs 2 and 3). These results place *Gli3* and *Plzf* function before cartilage differentiation.

Despite proximal patterning defects, *Gli3*$^{-/-}$;*Plzf*$^{-/-}$ limb-bud size is indistinguishable from that of wild types before E11.5, and only slightly smaller at E12.5 (Figs 2 and 3). We examined whether loss of proximal skeletal elements correlated with changes in expression of markers of limb growth and patterning (see Methods). *Fgf4*, *Fgf8*, *Gremlin*, *Hoxd9*, *Hoxd10* and *Hoxd11* all showed anteriorized expression similar to either *Gli3* or *Plzf* single mutants[8–10,11] (Supplementary Fig. 4). Although specific markers for P–D elements are unknown, *Meis1* and *Meis2* expression marks the proximal limb region[12]. These genes and other P–D markers such as *Hoxa9*, *Hoxa10* and *Hoxa11* are normally expressed in *Gli3*$^{-/-}$;*Plzf*$^{-/-}$ limbs (Fig. 4b and Supplementary Fig. 5). Thus, combined *Gli3* and *Plzf* function is required independently from proposed P–D markers.

As there are no other known markers for limb mesenchyme specification before *Sox9* expression, we investigated whether distinct cellular populations were affected by assessing cell proliferation and death (see Methods). Cell proliferation is not altered in *Gli3*$^{-/-}$;*Plzf*$^{-/-}$ limbs compared to the wild type at E10.5 (Fig. 4e). Strikingly, however, at E10.5 there is a small domain of cell death restricted to the most proximal region of *Gli3*$^{-/-}$;*Plzf*$^{-/-}$

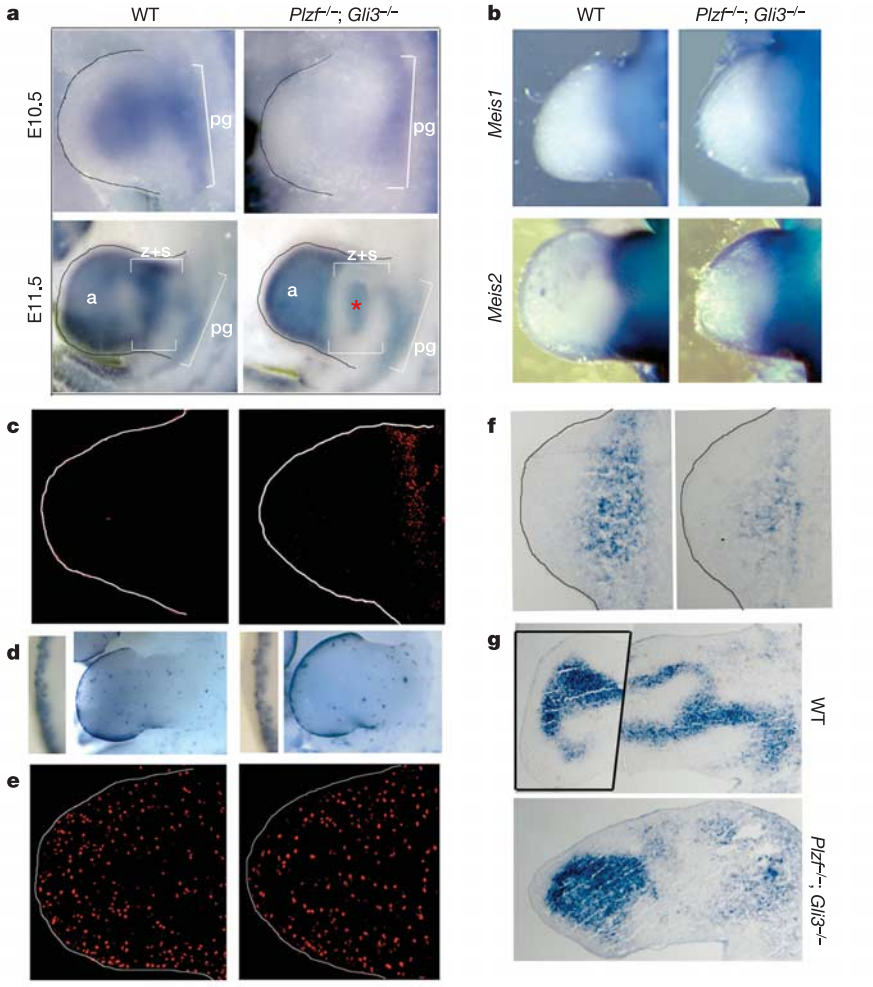

Figure 4 | Cellular consequences of *Plzf* and *Gli3* loss of function. **a**, *Sox9* messenger RNA expression in hindlimbs by whole-mount *in situ* hybridization. Red asterisk denotes small clump of Sox9-positive cells, which may relate to variable cartilage fragments in older *Gli3*$^{-/-}$;*Plzf*$^{-/-}$ hindlimbs. **b**, Expression of P–D markers as indicated at E10.5. **c**, **d**, TUNEL staining on E10.5 sections (**c**) and E11.5 whole-mounts (**d**). Note transient proximal cell death domain in E10.5 *Gli3*$^{-/-}$;*Plzf*$^{-/-}$ hindlimbs in **c**. Insets in **d**, magnification (×5) of apoptotic cells in the apical ectodermal ridge. **e**, Cell proliferation assayed by anti-phosphorylated histone H3 antibody at E10.5. No difference in cell proliferation was detected by quantifying percentage of mitotic cells to total nuclei in distal (wild type: 19%; *Gli3*$^{-/-}$;*Plzf*$^{-/-}$: 16.5%) and proximal (wild type: 15%; *Gli3*$^{-/-}$;*Plzf*$^{-/-}$: 18%) limb regions (average of 500 cells counted in each region). The limb-bud is highlighted by black or white outlining. **f**, *Bmpr1b* expression at E10.5 by section *in situ* hybridization. Note that *Bmpr1b*-positive cells are located similarly to the dying cells in *Gli3*$^{-/-}$;*Plzf*$^{-/-}$ hindlimbs (**c**) and this population is reduced in *Gli3*$^{-/-}$;*Plzf*$^{-/-}$ limbs. **g**, *Bmpr1b* expression at E11.5. Box in WT indicates overlay of the autopod from a serial section of the same hindlimb. Distal is to the left, posterior to the bottom.

hindlimb buds close to the body wall (Fig. 4c; $n = 2$). This cell death is transient, and at E11.5 no differences are detected between *Gli3*$^{-/-}$;*Plzf*$^{-/-}$ and wild-type limbs (Fig. 4d and data not shown for limb sections; $n = 4$). Importantly, the dying cells in *Gli3*$^{-/-}$;*Plzf*$^{-/-}$ hindlimbs reflect only a small fraction of proximal mesenchyme marked by *Meis* or *Sox9* expression in wild-type limbs (Fig. 4b and Fig. 4c), consistent with the normal size of *Gli3*$^{-/-}$;*Plzf*$^{-/-}$ hindlimbs (Fig. 2). Taken together, these results suggest that cells undergoing apoptosis in *Gli3*$^{-/-}$;*Plzf*$^{-/-}$ hindlimbs may reflect small cell populations required to correctly establish or organize the initial stylopod/zeugopod condensations, rather than the mesenchymal cells that contribute to their subsequent expansion. The fact that both *Gli3* and *Plzf* are initially expressed throughout the entire early limb-bud[8,10,13]indicates that these two transcription factors cannot, by themselves, be used as markers of these cells.

To further investigate the proximally restricted dying cells in *Gli3*$^{-/-}$;*Plzf*$^{-/-}$ limbs we examined expression of *Bmpr1b*, which marks cellular populations that prefigure the future limb cartilage primordium[14–16]. We identified a small group of previously unrecognized *Bmpr1b*-positive cells in the most proximal region of the E10.5 wild-type hindlimb (Fig. 4f), whereas these cells lie within the forelimb future stylopod region (Supplementary Fig. 6 and see ref. 13). Strikingly, in *Gli3*$^{-/-}$;*Plzf*$^{-/-}$ hindlimbs, *Bmpr1b*-positive cells overlap the apoptotic region and this population is greatly reduced (Fig. 4f). At E11.5, *Bmpr1b* expression clearly marks wild-type hindlimb stylopod, zeugopod and autopod primordia before histological condensation, whereas in *Gli3*$^{-/-}$;*Plzf*$^{-/-}$ hindlimbs, *Bmpr1b* is specifically absent in the stylopod/zeugopod region (Fig. 4g). Thus, a small subset of cells marked by *Bmpr1b* expression is critically affected at the earliest stages of limb development in *Gli3*$^{-/-}$;*Plzf*$^{-/-}$ embryos and correlates with subsequent loss of proximal skeletal elements (Fig. 3a). This suggests *Gli3* and *Plzf* are required to specify a subset of mesenchymal cells needed for the subsequent recruitment and formation of proximal condensations.

Our results demonstrate that *Gli3* and *Plzf* are specifically required for formation of stylopod and zeugopod elements at very early stages of limb development, before the initiation of cartilage condensations. These findings uncover a novel step regulated by *Gli3* and *Plzf* that is independent of known P–D markers and is required for establishing the correct timing and location of chondrocyte precursors specifically within proximal regions of the developing limb. Therefore, *Gli3* and *Plzf* cooperatively promote the proximal limb fate. However, as both *Gli3* and *Plzf* are broadly present throughout the developing limb without P–D bias in expression or activity, they cannot serve as markers of proximal limb identity[8,10,13,17]. We have also identified a requirement for *Gli3* function that appears to be independent of *Shh* signalling, because the defect is markedly different from *Shh*$^{-/-}$ limbs or from *Shh*$^{-/-}$;*Gli3*$^{-/-}$ limbs in which all skeletal elements are rescued[18-19].

Our studies provide a mouse model that directly addresses several unresolved questions in P–D limb patterning. First, our findings address whether P–D cartilage elements form via a branching mechanism[20,21]. The fact that distal structures form in *Gli3*$^{-/-}$;*Plzf*$^{-/-}$ limbs while proximal condensations are severely affected argues that P–D development relies on formation of individual condensations that are independently regulated. Second, *Gli3*$^{-/-}$;*Plzf*$^{-/-}$ limbs provide insight into how individual P–D cartilage condensations may be initiated. Previous studies suggest that the initial formation of condensations is dependent on the number of limb mesenchymal cells[7,22]. Importantly, despite gross alterations in proximal limb patterning, *Gli3*$^{-/-}$;*Plzf*$^{-/-}$ limb-bud size and mesenchyme cell number is normal before E11.5, and only slightly reduced at E12.5. Moreover, only a single proximal condensation that expresses joint markers is formed when the stylopod/zeugopod/joint cartilage template is evident in wild-type limbs. This raises the possibility that a separate population of joint precursors exists, or that a common joint/cartilage progenitor retains the ability to differentiate into proximal joints, but not into long bones, in *Gli3*$^{-/-}$;*Plzf*$^{-/-}$ limbs. Intriguingly, we identified a small population of *Gli3*- and *Plzf*-dependent *Bmpr1b*-positive cells present at the onset of limb development that may be required to establish initial cartilage condensations correctly. Therefore, although the overall number of mesenchymal cells is important for expansion of cartilage elements, *Bmpr1b*-positive cells may serve a distinct function necessary for formation of 'aggregation or organisation centres' to recruit cells from the surrounding mesenchyme into initial condensations, thus prefiguring the limb skeleton[15,20].

Our findings genetically demonstrate that the formation of proximal and distal skeletal patterning is differentially regulated very early in limb development. The finding that the autopod forms in the absence of the proximal elements, although overall limb size and P–D patterning is normal, is inconsistent with the idea of progressive specification raised by the Progress Zone Model[23]. In contrast, our findings are consistent with fate-mapping studies which propose that distinct P–D progenitor populations are specified early in an independent, non-progressive manner (Early Specification Model)[24]. Our results therefore extend and provide a genetic framework to test ideas proposed by these models.

METHODS

Animals. *Gli3*- and *Plzf*-deficient mouse embryos were obtained by intercrossing mice carrying the Gli3$^{Xt\text{-}J}$ allele[10] with mice carrying the targeted inactivation of *Plzf* (ref. 8) and genotyped as described[15,25].

Staining and whole-mount *in situ* hybridization. Alcian-blue and alizarin-red staining of cartilage and bone, and whole-mount *in situ* hybridization analyses were performed as described[8].

TUNEL and immunofluorescence assays. Apoptotic cells were detected *in situ* on frozen sections or in whole mount[26] by incorporating fluorescein-dUTP or Dig-11-dUTP, respectively, into fragmented DNA using terminal transferase according to the manufacturer's instructions (Roche Diagnostics). To detect cells in mitosis, a rabbit anti-phosphorylated histone H3 antibody (Upstate Biotechnology) and Cy-3 conjugated goat anti-rabbit IgG antibody (Jackson Lab) were used. Total nuclei were detected by DAPI staining (Jackson Lab) during the last wash of the immunofluorescence. Nonspecific antibody binding was blocked by incubating limb sections for 1 h at room temperature (25 °C) in PBT (PBS with 0.1% Tween-20) with 1% heat-inactivated goat serum (HIGS). All staining reactions were performed in PBT with 1% HIGS for 1 h at room temperature, except for incubation with primary antibody overnight at 4° C in a humidified chamber.

Received 12 January; accepted 6 May 2005.

1. Hall, B. K. & Miyake, T. All for one and one for all: condensations and the initiation of skeletal development. *Bioessays* **22,** 138–147 (2000).
2. Shubin, N., Tabin, C. & Carroll, S. Fossils, genes and the evolution of animal limbs. *Nature* **388,** 639–648 (1997).
3. Wright, E. *et al.* The Sry-related gene Sox9 is expressed during chondrogenesis in mouse embryos. *Nature Genet.* **9,** 15–20 (1995).
4. Akiyama, H., Chaboissier, M. C., Martin, J. F., Schedl, A. & de Crombrugghe, B. The transcription factor Sox9 has essential roles in successive steps of the chondrocyte differentiation pathway and is required for expression of *Sox5* and *Sox6*. *Genes Dev.* **16,** 2813–2828 (2002).
5. Davis, A. P., Witte, D. P., Hsieh-Li, H. M., Potter, S. S. & Capecchi, M. R. Absence of radius and ulna in mice lacking *hoxa-11* and *hoxd-11*. *Nature* **375,** 791–795 (1995).
6. Boulet, A. M. & Capecchi, M. R. Multiple roles of Hoxa11 and Hoxd11 in the formation of the mammalian forelimb zeugopod. *Development* **131,** 299–309 (2004).
7. Sun, X., Mariani, F. V. & Martin, G. R. Functions of FGF signalling from the apical ectodermal ridge in limb development. *Nature* **418,** 501–508 (2002).
8. Barna, M., Hawe, N., Niswander, L. & Pandolfi, P. P. Plzf regulates limb and axial skeletal patterning. *Nature Genet.* **25,** 166–172 (2000).
9. Barna, M. *et al.* Plzf mediates transcriptional repression of HoxD gene expression through chromatin remodeling. *Dev. Cell* **3,** 499–510 (2002).
10. Hui, C. C. & Joyner, A. L. A mouse model of greig cephalopolysyndactyly syndrome: the *extra-toesJ* mutation contains an intragenic deletion of the *Gli3* gene. *Nature Genet.* **3,** 241–246 (1993).
11. Masuya, H., Sagai, T., Moriwaki, K. & Shiroishi, T. Multigenic control of the localization of the zone of polarizing activity in limb morphogenesis in the mouse. *Dev. Biol.* **182,** 42–51 (1997).
12. Mercader, N. *et al.* Opposing RA and FGF signals control proximodistal

vertebrate limb development through regulation of Meis genes. *Development* **127,** 3961–3970 (2000).
13. Avantaggiato, V. *et al.* Developmental analysis of murine Promyelocyte Leukemia Zinc Finger (PLZF) gene expression: implications for the neuromeric model of the forebrain organization. *J. Neurosci.* **15,** 4927–4942 (1995).
14. Yi, S. E., Daluiski, A., Pederson, R., Rosen, V. & Lyons, K. M. The type I BMP receptor BMPRIB is required for chondrogenesis in the mouse limb. *Development* **127,** 621–630 (2000).
15. Pizette, S. & Niswander, L. BMPs are required at two steps of limb chondrogenesis: formation of prechondrogenic condensations and their differentiation into chondrocytes. *Dev. Biol.* **219,** 237–249 (2000).
16. Zou, H., Wieser, R., Massague, J. & Niswander, L. Distinct roles of type I bone morphogenetic protein receptors in the formation and differentiation of cartilage. *Genes Dev.* **11,** 2191–2203 (1997).
17. Wang, B., Fallon, J. F. & Beachy, P. A. Hedgehog-regulated processing of Gli3 produces an anterior/posterior repressor gradient in the developing vertebrate limb. *Cell* **100,** 423–434 (2000).
18. te Welscher, P. *et al.* Progression of vertebrate limb development through SHH-mediated counteraction of GLI3. *Science* **298,** 827–830 (2002).
19. Litingtung, Y., Dahn, R. D., Y., Fallon, J. F. & Chiang, C. *Shh* and *Gli3* are dispensable for limb skeleton formation but regulate digit number and identity. *Nature* **418,** 979–983 (2002).
20. Oster, G., Shubin, N., Murray, J. & Alberch, P. Evolution and morphogenetic rules: the shape of the vertebrate limb in ontogeny and phylogeny. *Evolution* **42,** 862–884 (1988).
21. Cohn, M. J., Lovejoy, C. O., Wolpert, L. & Coates, M. I. Branching, segmentation and the metapterygial axis: pattern versus process in the vertebrate limb. *BioEssays* **24,** 460–465 (2002).
22. Wolpert, L., Tickle, C. & Sampford, M. The effect of cell killing by x-irradiation on pattern formation in the chick limb. *J. Embryol. Exp. Morphol.* **50,** 175–193 (1979).
23. Summerbell, D. A. Quantitative analysis of the effect of excision of the AER from the chick limb-bud. *J. Embryol. Exp. Morphol.* **32,** 651–660 (1974).
24. Dudley, A. T., Ros, M. A. & Tabin, C. J. A re-examination of proximodistal patterning during vertebrate limb development. *Nature* **418,** 539–544 (2002).
25. Buscher, D., Bosse, B., Heymer, J. & Ruther, U. Evidence for genetic control of Sonic hedgehog by Gli3 in mouse limb development. *Mech. Dev.* **62,** 175–182 (1997).
26. Wakamatsu, Y., Mochii, M., Vogel, K. S. & Weston, J. A. Avian neural crest-derived neurogenic precursors undergo apoptosis on the lateral migration pathway. *Development* **125,** 4205–4213 (1998).

Supplementary Information is linked to the online version of the paper at www.nature.com/nature.

Acknowledgements We thank our laboratory staff, in particular S. Weatherbee and I. Zohn, for discussions; D. Ruggero for suggestions and support; and Y. Yang for discussions on joint formation. We thank Y. Yang, C. Tabin, D. Kingsley, A. Boulet, M. Capecchi and B. de Crombrugghe for *in situ* hybridization probes. This work was supported by the NIH (L.N.) and by a MSKCC Cancer Center Support grant. L.N. is an Investigator of the Howard Hughes Medical Institute.

Author Information Reprints and permissions information is available at npg.nature.com/reprintsandpermissions. The authors declare no competing financial interests. Correspondence and requests for materials should be addressed to L.N. (Lee.Niswander@uchsc.edu).